AIP Advances

RESEARCH ARTICLE | APRIL 03 2023

Underwater optical wireless communication system performance improvement using convolutional neural networks

Omar Nameer Mohammed Salim ; Salah A. Adnan ; Ammar Hussein Mutlag

Check for updates

AIP Advances 13, 045302 (2023)
https://doi.org/10.1063/5.0142823

CrossMark

View Online

Export Citation

Articles You May Be Interested In

Underwater optical wireless communication with subcarrier intensity modulation: an experimental demonstration

Proc. Mtgs. Acoust. (June 2021)

Enrichment of wireless data transmission based on visible light communication for triple play service application

AIP Conference Proceedings (January 2020)

Functional thermo-dynamics: A generalization of dynamic density functional theory to non-isothermal situations

J. Chem. Phys. (July 2013)

27 September 2023 11:31:04

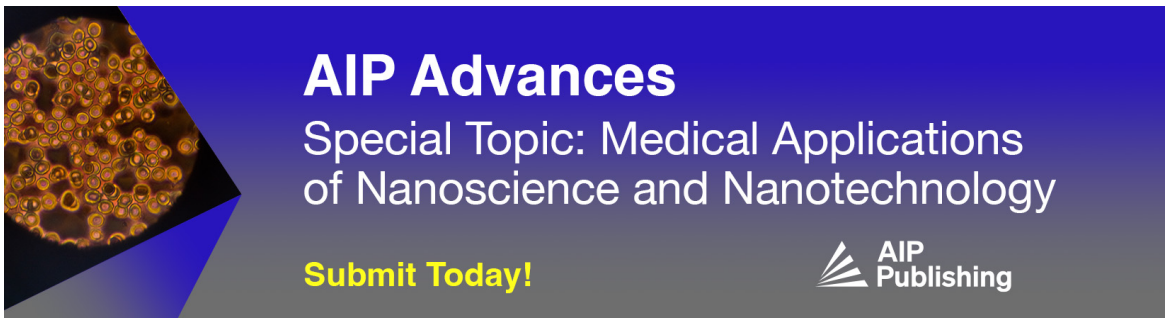

AIP Publishing

Underwater optical wireless communication system performance improvement using convolutional neural networks

Cite as: AIP Advances 13, 045302 (2023); doi: 10.1063/5.0142823
Submitted: 17 January 2023 • Accepted: 10 March 2023 •
Published Online: 3 April 2023

View Online Export Citation CrossMark

Omar Nameer Mohammed Salim,[1,2] Salah A. Adnan,[1,a)] and Ammar Hussein Mutlag[2]

AFFILIATIONS

[1] Laser and Optoelectronics Engineering Department, University of Technology-Iraq, Baghdad 10001, Iraq
[2] Electrical Engineering Technical College, Middle Technical University, Baghdad 10001, Iraq

[a)] Author to whom correspondence should be addressed: Salahaldeen.A.Taha@uotechnology.edu.iq

ABSTRACT

Many applications that could benefit from the underwater optical wireless communication technique face challenges in using this technology due to the substantial, varying attenuation that affects optical signal transmission through waterbodies. This research demonstrated that convolutional neural networks (CNNs) could readily address these problems. A modified CNN model was proposed to recover the original data of a non-return to zero on–off keying modulated signal transmitted optically through a tank full of Gulf seawater. A comparison between the proposed CNN model and a conventional fixed-threshold decoder (FTD) demonstrates the excellent performance of the proposed CNN model, which improved the bit error ratio (BER), signal-to-noise ratio (SNR), and effective channel length. The BER of the optical signals that are transmitted at powers of 24, 26, and 27 dBm and a bit rate of 10 Mbit/s at a distance of 3 m from the transmitter when FTD is used is 7.826×10^{-7}, 5.049×10^{-8}, and 8.38×10^{-10}, respectively. When the CNN decoder is used at the same distance and powers, the BER is 6.23×10^{-14}, 1.44×10^{-16}, and 2.69×10^{-18}, respectively. In conclusion, the BER decreased by about seven orders of magnitude, the effective channel length increased by four times, and the SNR decreased by about 20 dB. The simplicity of the proposed CNN decoder is independent of the prior knowledge of the channel conditions. Furthermore, the magnificent obtained results make the proposed CNN decoder an ideal substitute for ordinary underwater optical wireless communication decoders.

© 2023 Author(s). All article content, except where otherwise noted, is licensed under a Creative Commons Attribution (CC BY) license (http://creativecommons.org/licenses/by/4.0/). https://doi.org/10.1063/5.0142823

27 September 2023 11:31:04

I. INTRODUCTION

In recent years, underwater optical wireless communication (UOWC) technology has attracted increasing attention due to its high potential bandwidth and data rate.[1,2] UOWC is an attractive technology for marine communications, and its application may encourage the continued growth of sectors, including underwater wireless sensor networks, the undersea oil and gas industry, underwater drone vehicles, and ocean pollution monitoring.[3,4] UOWC can also support the development of new technologies that require reliable communication systems to expand their capabilities.[5] UOWC can potentially transmit data at rates comparable to those of optical fibers.[6] However, UOWC has the advantage of being a cable-free transmission method, where the data are delivered via light over a water channel.[7,8] Thus, UOWC can create more dynamic communication networks than optical fibers, leading to substantial cost reductions.[7,9] Furthermore, new UOWC networks can be deployed more easily than new optical fiber networks.[10] The high effect of seawater conductivity on the propagation of radio frequencies (RF) and the need for a complicated security system make UOWC preferable in underwater wireless networks.[5] However, in UOWC, data transfer takes place across a turbulent aquatic channel.[11] As the light beam passes through a turbulent oceanic channel, it will experience significant absorption, and random fluctuations would happen to the material's refractive index.[12] The amplitude and phase of the transmitted optical signal will thus change relative to these fluctuations.[13] These effects influencing the received light beam limit the performance of the UOWC systems and lead to considerable increases in

© Author(s) 2023

the bit error ratio (BER), which can often restrict the implementation of UOWC systems in real-world environments.[14] Therefore, there is a significant need to enhance underwater communication link performance without increasing the transmission power.[15]

Several previous publications have investigated various signal modulation methods that are suitable for improving UOWC systems.[16,17] Various studies have explored the possibility of using line coding to assist clock recovery at the receiver and remove low-frequency signal components. For example, on–off keying (OOK) modulation line coding, Manchester coding, 8B/10B line codes, and the 13B Baker code have all been presented as potential approaches to improve UOWC systems.[11,15,18,19]

Although the application of error-correcting codes has been extensively researched in the broader context of wireless optical communications, this aspect has received less attention in UOWC studies.[7] Some publications have proposed using Reed–Solomon (RS) codes as a physical layer-coding scheme to improve the BER, while others employ low-density parity-check codes.[20] In addition, a physical layer RS code and a data-link layer Luby transform code were used by Aqua Optical.[21] Transmitted data recovery at the receiver in the aforementioned techniques requires prior information regarding the encoder and decoder, in addition to detailed characterization of the channel condition information (CCI).[15,22] Since the conditions of oceanic underwater channels change frequently, it is costly and challenging to implement dynamic, reliable, standalone UOWC systems in natural environments. However, using convolutional neural networks (CNNs) for recovering transmitted data in UOWC systems is an effective potential solution to apply wireless optical systems in real-world oceanic channel environments without the need for *a priori* knowledge of the CCI.

The CNN approach is one of the most popular and widely used learning techniques in the deep learning (DL) computing paradigm.[23] DL networks can train themselves and learn the relationship between a system's inputs and outputs, thereby allowing them to optimize the performance of an entire system and learn how its inputs and outputs are related.[24–26] DL has excellent functional characteristics, including robustness, generalization, and scalability, making it suitable for a wide range of modern applications.[23] In recent years, DL has become highly prevalent in research and extensively applied in a variety of scenarios.[27,28] These include image classification, spam exposure, text recognition, and search recommendations.[29] In addition, researchers have successfully used DL in wireless communication systems, such as in channel estimation encoding–decoding and modulation discrimination.[24,30] Incorporating DL into wireless communication systems can boost their overall performance due to the ability of DL to train a wide range of complex models using a set of standardized methods and tools.[31,32] All of these models employ various forms of training and learning to boost the efficiency of the communication system as a whole.[23] In addition, in a communications context, DL has been employed in orthogonal frequency-division multiplexing as a means of alleviating the peak-to-average power ratio problem, channel estimation, and signal detection.[33,34]

Furthermore, CNNs have found numerous uses in the realm of optical communication systems, including in fiber-induced nonlinear mitigation, identifying modulation formats in coherent digital receivers, and reducing the computational complexity of various optical communication tasks.[35,36] Furthermore, in free space optical communication (FSO), CNNs have been demonstrated as an effective approach for detecting atmospheric turbulence, developing adaptive techniques for orbital angular momentum, and correcting sensorless systems.[37–39] Researchers have also proposed DL as a possible solution to problems involving a lack of complete channel information in correlated FSO channels.[40,41]

In this research context, in this study, we propose a new method for detecting signals transmitted in an underwater channel; specifically, we suggest a CNN model as an efficient decoder substitute for the OOK decoder based on a threshold value. To verify the proposed model, we generate a pseudo-random bit sequence (PRBS) data stream and OOK modulation. The generated modulated signal was transmitted via a 520-nm laser diode (LD) through a Gulf seawater channel. We evaluate the performance of the proposed CNN model by comparing its results with those of an accurate fixed-threshold OOK decoder. This comparison highlights significant improvements in the detection of OOK-modulated signals when the proposed CNN model is used.

The rest of this research is organized as follows: In Sec. II, optical wireless communication in the underwater channel has been reviewed and discussed. The CNN architectures and the proposed CNN model are shown in Sec. III. The results and discussions are provided in Sec. IV. Finally, in Sec. V, the research has been concluded.

II. OPTICAL SIGNAL TRANSMISSION IN WATER

UOWC is a communication technology based on transmitting data via light through a water channel. In this study, non-return to zero (NRZ) OOK intensity modulation of laser light with a direct detection method using a silicon photomultiplier (SiPM) was adopted. The optical signal received by the SiPM after underwater propagation can be described by the following equation:[42]

$$S_{R-K} = \Re_{SiPM} h_K S_{T-K} + n_K, \tag{1}$$

where $\Re_{SiPM}$ denotes the responsivity of the SiPM, represented by[43]

$$\Re_{SiPM} = \frac{\eta_{PD} \cdot \lambda \cdot \mathrm{G} \cdot \mathrm{e} \cdot (1 + \mathrm{P}_{AP}) \cdot (1 + \mathrm{P}_{XT})}{\mathrm{h} \cdot \mathrm{C}}, \tag{2}$$

where η_{PD} and G denote the SiPM photon detection efficiency and gain, respectively. In addition, h, C, λ, e, P_{XT}, and P_{AP} denote the Planck constant, speed of light, wavelength of the incident light, elementary charge, crosstalk probability, and after-pulsing probability, respectively. The term h_K in Eq. (1) denotes the status coefficient of the channel, which includes attenuation due to water turbulence and the interaction of light photons with water molecules and other dissolved particles in the water, which lead to absorption and scattering of the transmitted light signal. Thus, h_K must include the total effects of the water channel,[44]

$$h_k = P_{R-K} \big/ P_{T-K}, \tag{3}$$

where $P_{R\text{-}K}$ and $P_{T\text{-}K}$ are the received and transmitted optical power, respectively. As shown by Eq. (3), h_k is a random variable that depends on the water channel properties and turbulence. The transmitted optical signal that is modulated using OOK-NRZ with average optical power $P_{T\text{-}K}$ is denoted in Eq. (1) by $S_{T\text{-}K}$, $k \in \{0, 1\}$; this

27 September 2023 11:31:04

© Author(s) 2023

parameter takes the value of $P_{T\text{-}0}$ for the transmission of a "0" bit and $P_{T\text{-}1}$ for the transmission of a "1" bit. The term n_K in Eq. (1) symbolizes the SiPM photo-current noise, which includes thermal noise, dark current noise, signal shot, and background noise. The dark current of the SiPM is represented by[43]

$$I_D = e \cdot G \cdot DCR(1 + P_{XT} + P_{AP}), \tag{4}$$

where DCR denotes the dark count rate of the SiPM. The sum of the sources of noise variance is represented by[45,46]

$$\sigma^2_{t-nK} = \sigma^2_T + (\sigma^2_{D-n} + \sigma^2_{B-n} + \sigma^2_{SS-n}K)R^2_L. \tag{5}$$

Here, $\sigma^2_T, \sigma^2_{D-n}, \sigma^2_{B-n}, \sigma^2_{SS-nK}, R^2_L$ symbolize the variance of the thermal noise, dark noise, background noise, and signal shot noise and the load resistance of the transimpedance amplifier, respectively. $\sigma^2_T, \sigma^2_{D-n}, \sigma^2_{SS-nK}$ are given by[45]

$$\sigma^2_T = 4K_Z TBR_{\mathrm{L}}, \quad \sigma^2_{D-n} = 2eGFBI_{\mathrm{d}}, \quad \sigma^2_{SS-nK} = 2eGFBI_{SK}, \tag{6}$$

where K_Z, T, B, F, and I_{SK} represent the Boltzmann constant, receiver equivalent temperature, receiver low-pass filter bandwidth, SiPM excess noise factor, and detected signal current, respectively. Although the variation in the signal-induced shot noise is dependent on the transmitted optical power, i.e., ($P_{T\text{-}0}$ or $P_{T\text{-}1}$), this variation also depends on the channel coefficient h_K. For accurate signal detection, a comparison of the received signal $S_{R\text{-}K}$ with the predetermined threshold γ_{th} is required. The average BER of the link is calculated as[47]

$$P_K = \int_0^{\infty} P_K(e \mid h_K) f_h(h_K) dh, \tag{7}$$

where $P_K(e \mid h_K)$ is the instantaneous BER contingent on h_K and $f_h(h_K)$ is the probability function of h_K. From Eqs. (1), (5), and (6), the instantaneous BER related to the status coefficient of the channel can be found using the following equation:[48]

$$P_K(e|h_K) = \frac{1}{4}\,\mathrm{erfc}\left(\frac{\gamma_{th} - S_0}{\sqrt{2\sigma^2_{t-n0}}}\right) + \frac{1}{4}\,\mathrm{erfc}\left(\frac{S_1 - \gamma_{th}}{\sqrt{2\sigma^2_{t-n1}}}\right). \tag{8}$$

Here, S_0, S_1 denote the input signals to the demodulator corresponding to "0" and "1" bits, respectively, where S_0, S_1 are given by[49]

$$\begin{aligned} S_0 &= R_L(R_{SIPM} S_{T-0} h_K + I_D), \\ S_1 &= R_L(R_{SIPM} S_{T-1} h_K + I_D). \end{aligned} \tag{9}$$

In addition, σ_{t-n0} and σ_{t-n1} denote the total noise variance values corresponding to "0" and "1" bits, respectively. To minimize the BER, the optimal threshold value γ_{op-th} must be calculated, given an accurate estimation of CCI, where γ_{op-th} is given by[44]

$$\gamma_{op-th} = \frac{S_0\sigma^2_{t-n1} - S_1\sigma^2_{t-n0}}{\sigma^2_{t-n1} - \sigma^2_{t-n0}} + \left[\frac{S_1^2\sigma^2_{t-n0}}{\sigma^2_{t-n1} - \sigma^2_{t-n0}} + \left(\frac{S_0\sigma^2_{t-n1} - S_1\sigma^2_{t-n0}}{\sigma^2_{t-n1} - \sigma^2_{t-n0}}\right)^2 - \frac{S_0^2\sigma^2_{t-n1}}{\sigma^2_{t-n1} - \sigma^2_{t-n0}} - \frac{\sigma^2_{t-n0}\,\sigma^2_{t-n1}}{\sigma^2_{t-n1} - \sigma^2_{t-n0}} \ln\left(\frac{\sigma^2_{t-n0}}{\sigma^2_{t-n1}}\right)\right]^{0.5}. \tag{10}$$

As shown in Eq. (10), the optimal threshold depends on the status coefficient of the channel, which implies that to achieve the optimum BER value, the receiver must continuously and accurately estimate variations in h_K values and adjust γ_{th} according to those values. Since the properties and conditions of the underwater ambient change frequently, the process of designating accurate h_K values will be very costly and requires complicated, time-consuming methods.

III. UNDERWATER WIRELESS OPTICAL COMMUNICATION

A schematic diagram of the UOWC system is shown in Fig. 1. In this configuration, a 520-nm LD is used to transmit the data signal through a seawater channel. A SiPM is used to detect the transmitted optical signal and convert it to an electrical signal. The optical signal transmitted in an underwater channel suffers from strong attenuation related to the properties of that channel.

Subsection III A will discuss the characteristics of the proposed underwater channel and the propagation of optical signals through it. In addition, the implemented experimental UOWC system will be described thereafter.

A. Experimental UOWC system setup

In the experimental UOWC system setup, a water tank with a width of 1.25 m, height of 1 m, and length of 8 m, constructed in an outdoor area, was used to simulate an underwater channel. The tank was filled with Gulf seawater collected from Al-Faw town, Basra, Iraq. The experimental UOWC system, shown in Fig. 1, is based on a 520-nm LD (Thorlabs-L520G1) as an optical source.

The beam of the selected LD has a 25° perpendicular divergence angle and a 7.5° parallel divergence angle. This wide divergence angle of the laser beam leads to a beam spot with approximately 4 m diameter at a distance of 8 m from the transmitter in the perpendicular axis. Therefore, a compact collimating system consisting of a 16 mm plano-convex lens and a cylindrical lens fastened in a metal case was used to reduce the divergence angle. The LD and collimating system were attached to a metal housing. Since the LD in this work operates at powers of up to 28.5 dBm, an efficient proportional integral derivative-controlled cooling system was also used.[50]

A PRBS11 OOK-NRZ signal is generated in MATLAB and then loaded into the arbitrary waveform generator. The LD modulation is performed by combining the generated signal with a DC biasing voltage from a controlled LD driver power supply through Mini-Circuits' ZFBT-4R2GW bias tee. The collimating system collimated the modulated optical signal and transmitted it to the Gulf seawater channel through a fine 4-mm-thick glass window.

At the receiver, the transmitted optical signal is detected and converted to an electrical signal by a SiPM (MICROFC–SMTPA–30035) after passing through a plano-convex lens that focuses the optical beam toward the SiPM. To minimize background noise, the experiments were conducted at night in the absence of any artificial light source. The ambient light recorded during the experiment was around −30 dBm. The electrical signal from the SiPM module was captured using a digital storage oscilloscope and transferred to a computer. Then, the received signals were processed using MATLAB, with two scenarios adopted to analyze the data and calculate the BER. The first scenario was based on an accurate

27 September 2023 11:31:04

© Author(s) 2023

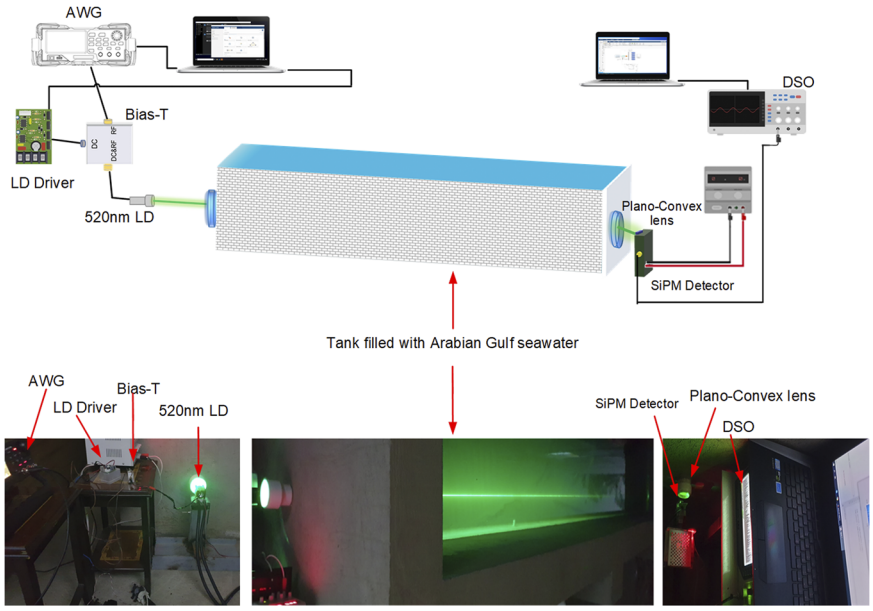

FIG. 1. Schematic diagram of the UOWC system.

threshold OOK-NRZ decoder, while the second was based on the proposed CNN model.

B. Experiment data collection

The UOWC system described above was implemented and operated. Before data collection, the transmissivity of the optical elements at the transmitter (i.e., the collimating system and the glass window) was calculated, yielding a value of around 77%. Based on the transmissivity of the optical elements, the LD was adjusted to emit the modulated signal at three different optical powers (24, 26, and 27 dBm), where the net optical powers of the transmitted signals, after ensuring that the optical elements are suited to these power values.

The attenuation coefficient of the Gulf seawater used to fill the experiment tank, measured at a wavelength of 520 nm without turbulence, was found to equal 1.467 m^{-1}. The channel power loss as a function of channel length for the three transmitted power cases is shown in Fig. 2.

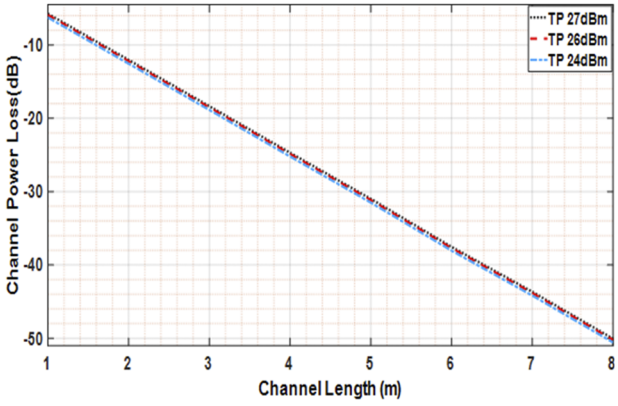

FIG. 2. Channel power loss as a function of channel length for three values of transmitted power (24, 26, and 27 dBm).

The PRBS11 OOK-NRZ signal was transmitted in the Gulf seawater channel at bit rates of 10, 30, and 60 Mbit/s. The transmitted optical signal was received and converted to an electrical signal by the SiPM, and the electrical signals were then transferred to a computer using an interfaced oscilloscope. Processing in MATLAB was then performed to extract the PRBS11 digital data transmitted through the underwater channel. In this study, data were collected for 72 signals that were transmitted through the Gulf seawater channel. Data were collected every 1 m along the underwater channel, including those for transmitted optical power and the transmitted bit rate value. The collected data were then processed and analyzed using the accurate fixed-threshold decoder (FTD) and the proposed CNN model to extract the digital data information.

IV. PROPOSED CNN MODEL FOR THE UOWC SYSTEM

In this research, an innovative UOWC decoder for OOK-NRZ signals was proposed. The essential concept of the proposed method is that a CNN model can be used as an effective decoder instead of the traditional FTD. The CNN algorithm is the most well-known and commonly used algorithm in the DL field. Compared to other algorithms, the primary advantage of CNNs is that they can identify significant features automatically without the need for any kind of supervision from humans. Hence, CNN models have been used in a wide variety of stand-alone applications such as face and speech processing, computer vision, and customer preference recognition.

A. CNN structure

The structure of CNNs is inspired by neurons in animals and human brains; specifically, the CNN structure sequence simulates the sequence of complex cells that form the visual cortex in a cat's

27 September 2023 11:31:04

© Author(s) 2023

brain.[51] The CNN systems typically consist of three main layers, i.e., an input layer, a hidden layer, and an output layer, as shown in Fig. 3.

The hidden layer comprises multiple convolution layers preceding the sub-sampling (pooling) layer and the fully connected (FC) layers.[52] A CNN is a feedforward (FF) neural network, i.e., the information traverses the network from the input layer to the output layer through the hidden layer in the forward direction only.[35]

In CNN models, the input I of layers is organized in a three-dimensional array of size height (h) × width (w) × depth (d), where h is equal to w and d represents the channel dimension.[23] In a red-green-blue (RGB) image, for instance, d equals 3. Each convolutional layer can use various filters (kernels, represented by k) with dimensions $m \times m \times l$, where m is less than h and l is less than or equal to d.[51] The kernels serve as a basis for local connections, each of which uses the same kernel-specific parameters (bias B^k and weight W^k) to produce k feature maps h^k when convolved with the input. The dot-product between the input and weights is computed by the convolution layer, and the activation function is then applied to the convolution layer output, as described by

$$h^k = f\left(W^k * x + B^k\right). \tag{11}$$

At this stage, all feature maps in the sub-sampling layers must be down sampled. Accordingly, the network parameters will be reduced, allowing the overfitting issues to be addressed and accelerating the training process.[24] The pooling function (such as global or minimum) for each feature map is applied to an adjacent area. In terms of the kernel size P, the adjoining size equals $P \times P$. Eventually,

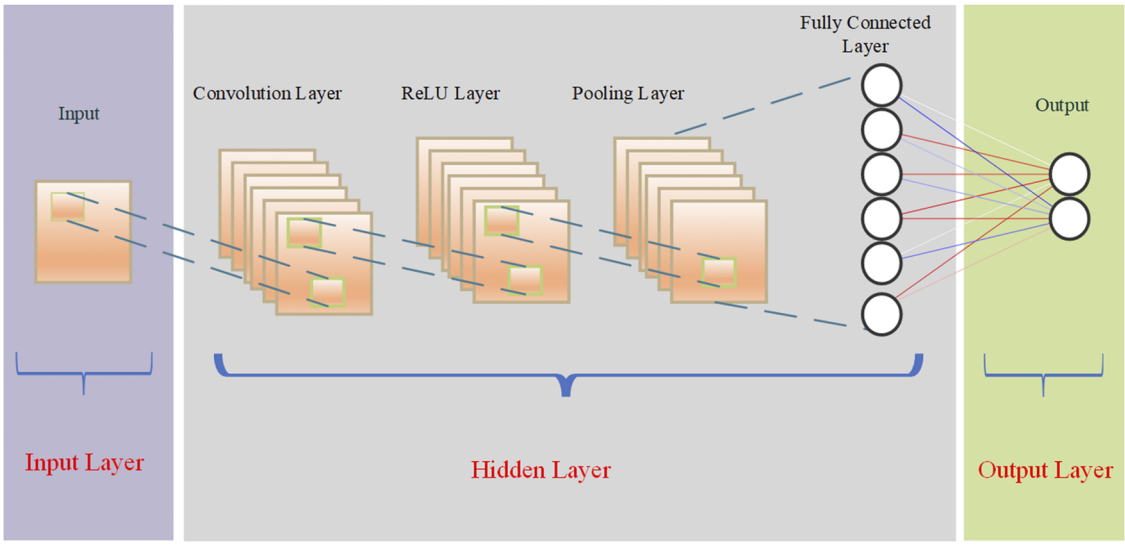

FIG. 3. CNN structure.

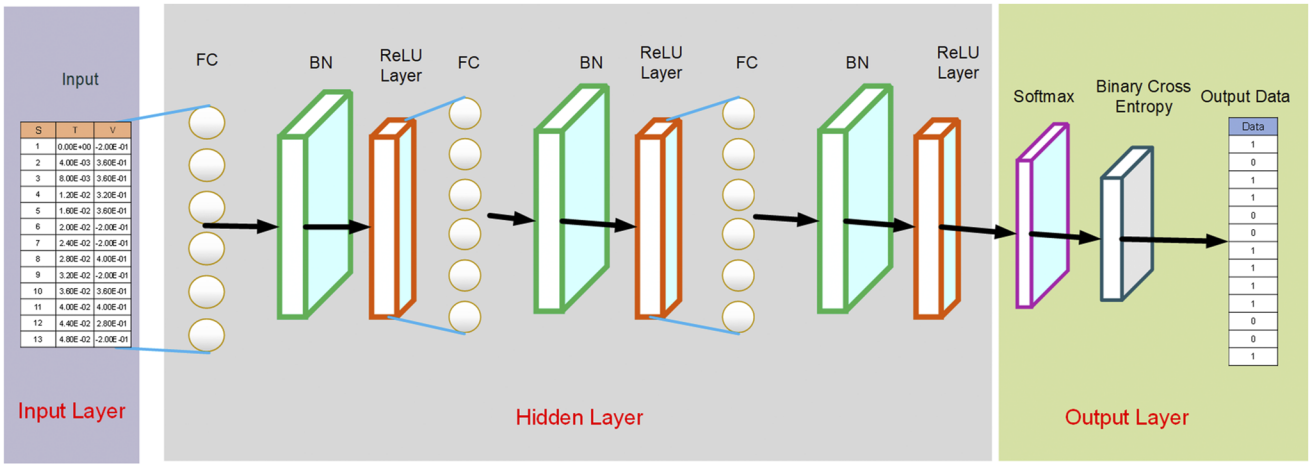

FIG. 4. Proposed CNN model.

© Author(s) 2023
27 September 2023 11:31:04

TABLE I. Hyperparameters of the proposed CNN model.

CNN model hyperparameters	Value
No. of epochs	3000
Batch size	512
Learning rate	0.0005
Optimizer	Adam
FC layer 1 nodes	256
FC layer 2 nodes	96
FC layer 3 nodes	96

the FC layers are responsible for creating the high-level abstraction based on the received mid- and low-level data. The end layer is used in the process of generating classification scores: when referring to a particular case, each score denotes the probability of a particular class.

B. Proposed DL-CNN model

As detailed above, the proposed detection method is based on the CNN model for OOK-NRZ modulation to enable the use of wireless optical communication in various underwater channels without the need for *a priori* knowledge of the channel properties. The CNN detection model was proposed to replace the accurate fixed-threshold OOK-NRZ decoder, which is required to receive the OOK-NRZ modulated signal and recover the original data with a minimum BER. The operation of the CNN model consists of two distinct stages. The training procedure represents the first stage of the process, during which a dataset is inputted and the CNN system performs iterative training and learning to reconstruct the original data. When this procedure is complete, the system will save the process weight if it successfully minimizes the loss. After the completion of the training procedure, in the second stage, the CNN system can then receive and process new OOK-NRZ modulated signals that are transmitted in the underwater channel and are accordingly affected by noise. The weights that were saved at the end of the training procedure are utilized by the CNN model to predict the received data.

The dataset collected for this research includes data bits of 72 vectors of transmitted signals through the Gulf seawater. Each of these vectors has a data size of 1 Mbit. The training and testing data for the CNN algorithm comprise features that are ready to be processed by the classification layers contained inside the algorithm; therefore, the feature extraction process is not required for the CNN model proposed herein.

The dataset was divided randomly into three sets: a training set, which comprises 70% of the original dataset, and validation and testing sets, each of which contains 15% of the original dataset. Since the feature extraction is not required in the proposed CNN model, the convolutional and pooling layers can be removed. This layer reduction will reduce processing operation, training time, and

27 September 2023 11:31:04

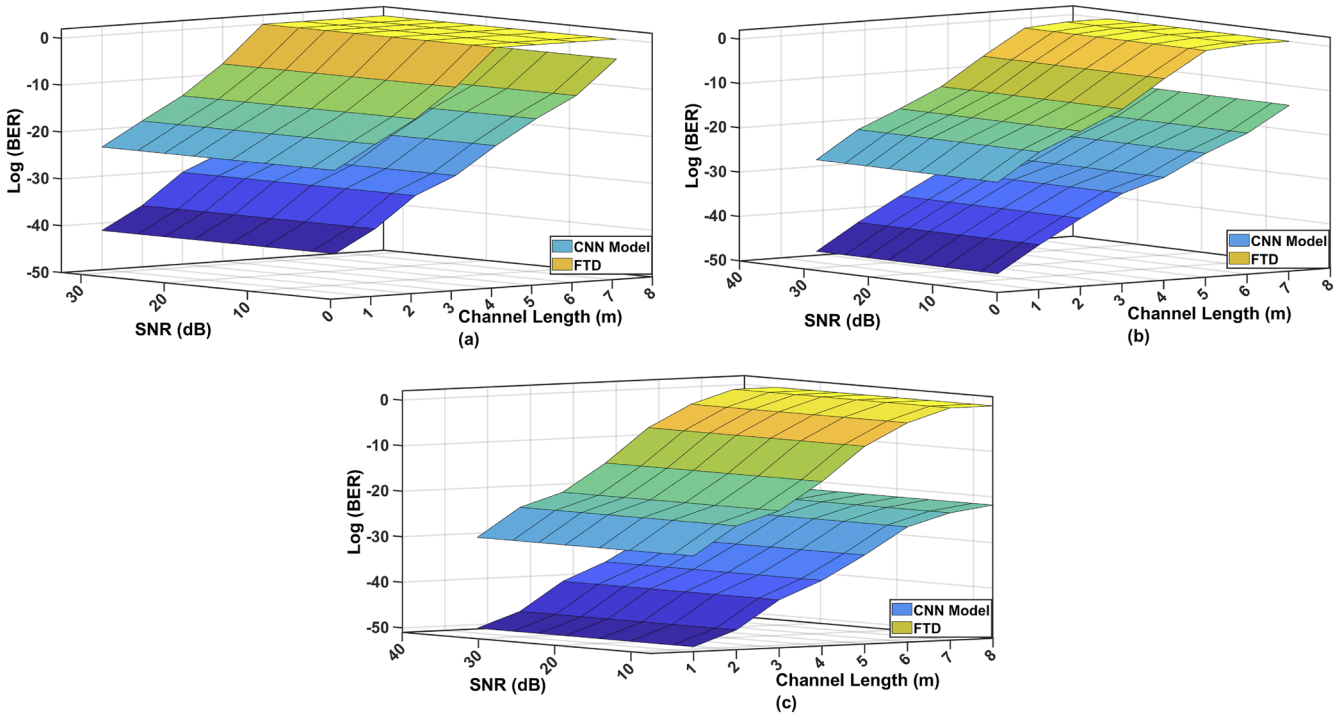

FIG. 5. BER performance against channel length and SNR when FTD and proposed CNN models are used for a signal with a bit rate of 10 Mbit/s and transmitted power of (a) 24 dBm, (b) 26 dBm, and (c) 27 dBm.

© Author(s) 2023

computational hardware requirements. The structure of the proposed CNN model is shown in Fig. 4, where the input layer is combined directly with the FC layer connected to the batch normalization (BN) layer.

The Rectified Linear Unit (ReLU) activation function is expressed as

$$f_{ReLU}(x_i) = \max(0, x_i). \tag{12}$$

The ReLU function is used in the proposed model after each BN layer. The set comprising the FC layer, BN layer, and ReLU activation function in the hidden layer is repeated three times and then connected to the Softmax (SM) activation function in the output layer,

$$f_{SM} = \frac{e^{x_i}}{\sum_{j=1}^{k} e^{x_j}}. \tag{13}$$

The SM activation function converts the output data value from the hidden layer to values from 0 to 1. The binary cross entropy (i.e., log loss) function is used at the end of the proposed CNN model to make a comparison between the predicted bit values (0 or 1) and the original transmitted data bit values.

V. RESULTS AND DISCUSSION

In this work, OOK-NRZ optical signals were transmitted in a tank filled with Gulf seawater to allow the performance of the proposed CNN model to be impartially evaluated. Signals transmitted through the seawater channel were received and converted to electrical signals using a SiPM. The electrical signals inputted to the decoder contained both the modulated data and noise. Two methods were used to decode the detected modulated signals and extract the originally transmitted data. The first method is based on a fixed accurate threshold value determined by practically adjusting its value according to the CCI until an optimum value is reached. The adopted threshold value is used to determine whether the received bit is 1 or 0—if the received value is equal to or greater than the threshold value, then the detected bit is classified as 1; otherwise, the received bit is 0. The second method used to decode the detected signals is based on the proposed CNN model described in Sec. IV B. After multiple attempts to optimize the CNN model hyperparameters, the training process variables were set. Table I shows the optimum CNN hyperparameters chosen based on a balance between the model accuracy and computational processing time and complexity.

The BER values of the received signal data extracted using the FTD and the proposed CNN model are shown in Figs. 5–7, which show the BER of 520-nm optical signals transmitted at bit rates of 10, 30, and 60 Mbit/s, respectively, at power values of 24, 26, and 27 dBm against channel lengths and the SNR.

As shown in Fig. 5(a), the BER increases significantly as the distance between the transmitter and receiver increases due to the strong attenuation of the Gulf seawater. The BER for the FTD method does not achieve the minimum acceptable (MA) BER of

27 September 2023 11:31:04

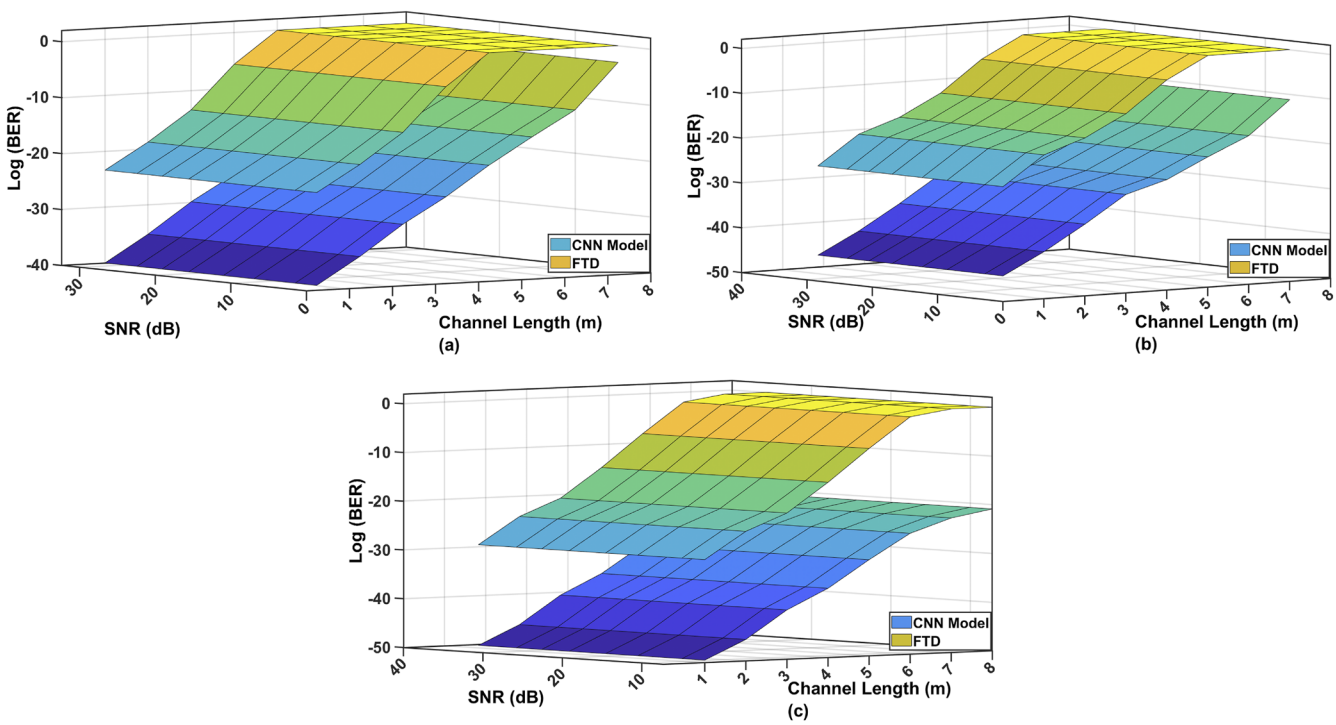

FIG. 6. BER performance against channel length and SNR when FTD and proposed CNN models are used for a signal with a bit rate of 30 Mbit/s and transmitted power of (a) 24 dBm, (b) 26 dBm, and (c) 27 dBm.

© Author(s) 2023

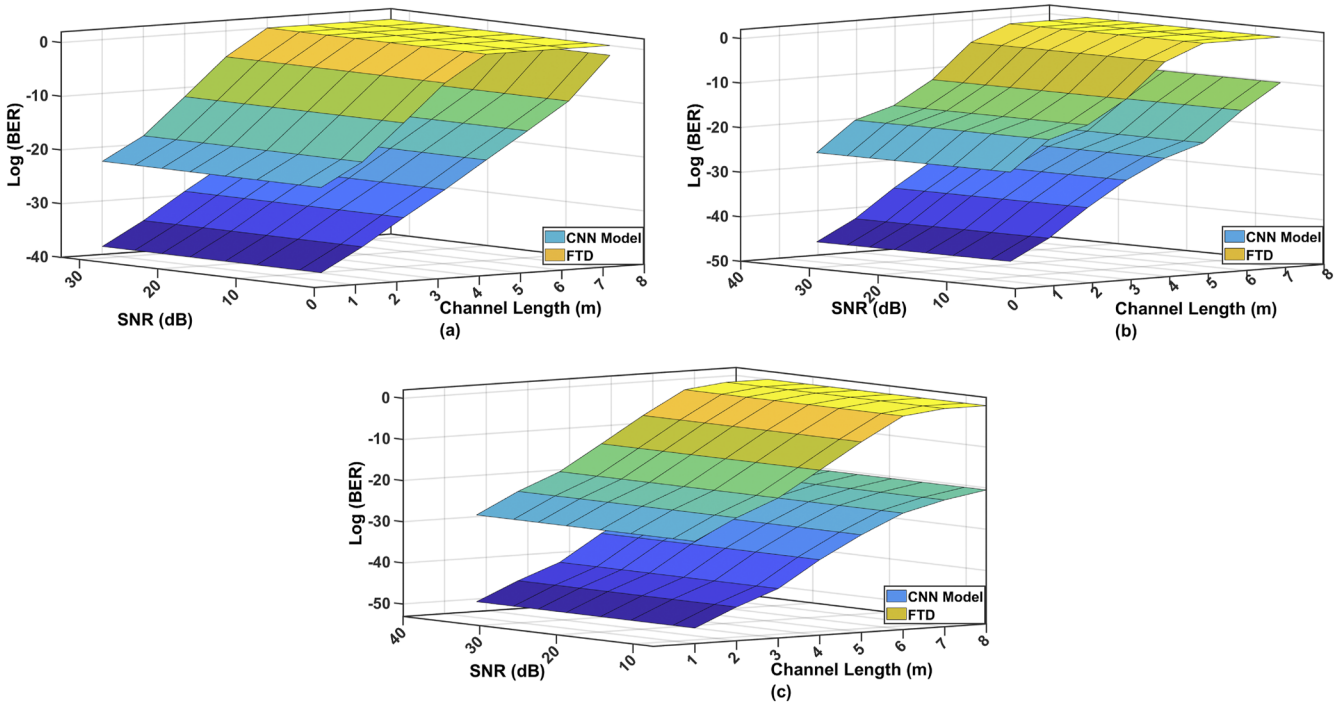

FIG. 7. BER performance against channel length and SNR when FTD and proposed CNN models are used for a signal with a bit rate of 60 Mbit/s and transmitted power of (a) 24 dBm, (b) 26 dBm, and (c) 27 dBm.

10^{-9} at a channel length of 3 m when transmitting with an SNR of 24.8 dB. As shown in Figs. 5(a)–5(c), when the BER for the FTD decoder at a distance of 3 m and transmitting at a bit rate of 10 Mbit/s is 7.826×10^{-7}, 5.049×10^{-8}, and 8.38×10^{-10}, the only value falling within the MA-BER is when transmitting at 27 dB. When the transmitted bit rate is 30 Mbit/s, the BER is 1.466×10^{-6}, 7.375×10^{-8}, and 1.400×10^{-9}, as shown in Figs. 6(a)–6(c). However, Figs. 7(a)–7(c) show that the BER is 8.24×10^{-6}, 8.50×10^{-8}, and 5.79×10^{-9} when transmitting at a bit rate is 60 Mbit/s. The presented samples of the BER in Figs. 5–7 exhibit that at a distance of 3 m from the transmitter, the MA-BER is achieved only when transmitting at a bit rate of 10 Mbit/s and a power of 27 dBm. Hence, to achieve the MA-BER at a channel length of 3 m or higher when using the FTD method, signals must be transmitted with an SNR exceeding 26.7 dB, as shown in Figs. 5(b) and 5(c). Similarly, to achieve the MA-BER at a 3 m channel length, as shown in Fig. 6, the signals must be transmitted with an SNR exceeding 26.9 dB. As shown in Fig. 7, the SNR required for the transmitted signals is greater than 27.2 dB. These observed differences in the required SNR values are due to the increasing bit rate. The high SNR values needed to achieve a reliable UOWC channel when the conventional FTD method is used affect the maximum channel length and bit rate that can be practically achieved, in addition to the high cost and challenging implementation of such a system.

The BER values of the data of the received signals extracted using the proposed CNN model are also shown in Figs. 5–7. As shown, the proposed CNN model achieves BER values less than those of achieved by the conventional FTD method. A shown in Figs. 5(a)–5(c), at the distance of 3 m from the transmitter, the BER of the data of received signals is 6.23×10^{-14}, 1.44×10^{-16}, and 2.69×10^{-18}. When the transmitted bit rate is 30 Mbit/s, as shown in Figs. 6(a)–6(c), the BER is 1.09×10^{-13}, 3.26×10^{-16}, and 4.68×10^{-18}, and when the transmitted bit rate is 60 Mbit/s, as shown in Figs. 7(a)–7(c), the BER is 7.66×10^{-16}, 2.4×10^{-13}, and 1.59×10^{-17}. The obtained values of the BER when the proposed CNN decoder is used achieve the MA-BER at a channel length of 3 m. It is also shown that the proposed CNN decoder when extracting data from the received signals transmitted in the Gulf seawater channel requires 7.4 dB as the minimum SNR value to achieve the MA-BER; thus, the transmitted SNR values for the proposed CNN model are around 20 dB lower than those needed for the conventional FTD method.

The effective communication channel length also increased, as shown in Fig. 8. The effective channel length under the MA-BER condition extended from 1.8 m when the FTD method was used to 5 m when the proposed CNN model was used at a transmitted optical power of 24 dBm, as shown in Fig. 8(a). In addition, for optical powers of 26 and 27 dBm, the channel lengths increased from 2 to 3 m when the FTD method was used to 6.8 and 8 m when the proposed CNN model was used [Figs. 8(b) and 8(c)]. Based on these results, the effective channel length increases approximately fourfold when the proposed CNN model is used.

Summarization of the recent experimental UWOC systems with different optical sources, data rates, water types, and transmis-

27 September 2023 11:31:04

© Author(s) 2023

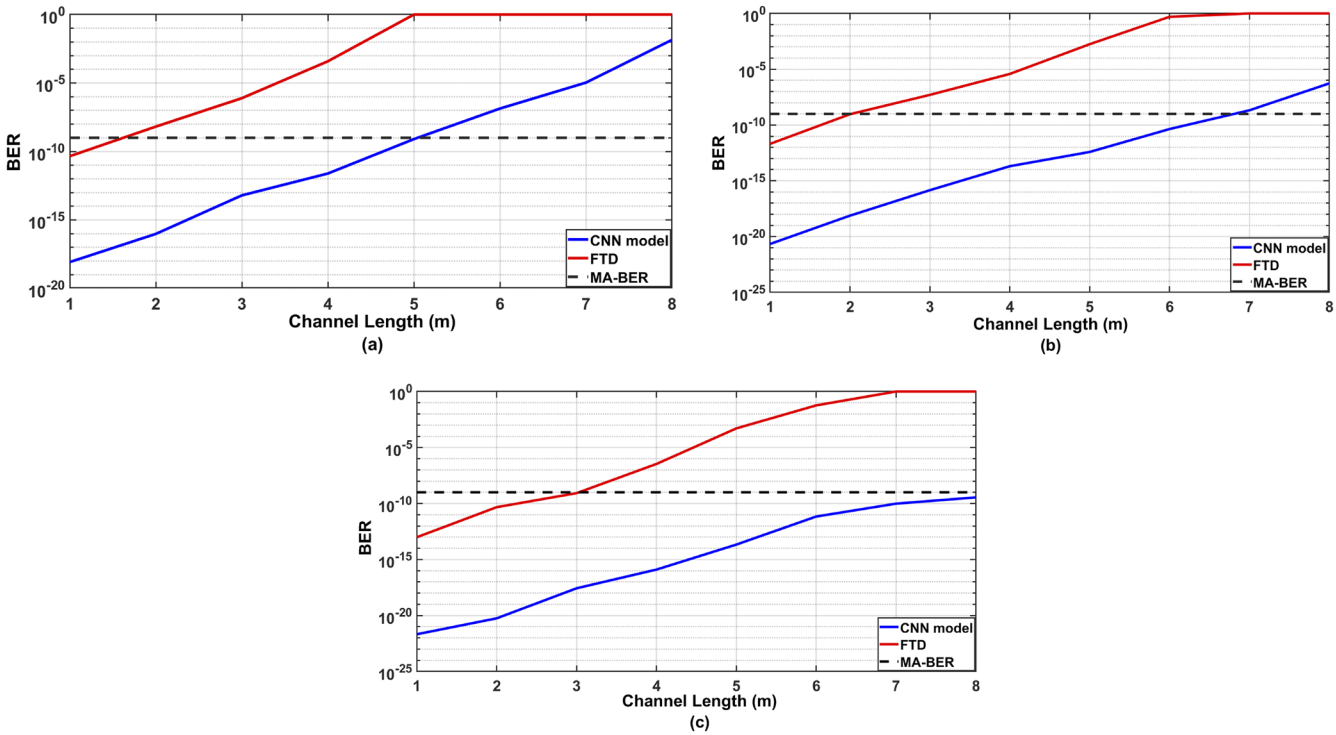

FIG. 8. Effective channel length that meets the MA-BER condition for three values of transmitted power: (a) 24 dBm, (b) 26 dBm, and (c) 27 dBm.

TABLE II. Comparison of recent experimental UWOC systems.

Research group	Optical source type	Detector type	Data rate Mbit/s	Water type	BER	Detection improvement method
P. Tian *et al.*[6]	440 nm LED array 1.8 dBm	APD	200	Tap-water	3×10^{-6}@5.4 m	OFDM & fixed threshold
J. Wang *et al.*[5]	520 nm LD, 9 dBm	APD	400	Tap-water	1.2×10^{-4}@80 m	Nonlinear equalization
X. Tang *et al.*[17]	532 nm laser, 1 dBm	APD SiPM	200	Tap-water	4.1×10^{-2}@1.6 m 5.3×10^{-4}@1.6 m	DPSK & forward error correction
Z. Chen *et al.*[14]	520 nm LD, 9 dBm	SiPM	20	Water with maalox solution	2.5×10^{-6}@24 m	Forward error correction
H. Yang *et al.*[12]	450 nm LED	SPAD	1	Seawater Jerlov II	5.5×10^{-4}@1.5 m	Deep learning
This work	520 nm LD, 27 dBm	SiPM	10 30 60	Seawater Jerlov 5C	4.2×10^{-10} 9.2×10^{-11} 6.4×10^{-11}@8 m	CNN decoder

sion distances and the comparison with this work are carried out as shown in Table II.

VI. CONCLUSION

Due to the strong attenuation and turbulence of underwater communication channels, the performance of UOWC systems depends strongly on the detection devices and methods used. In this study, a SiPM detector was used in the receiver; the characteristics, performance, and advantages of this detector type make it the optimal choice at present for UOWC applications. A CNN model was proposed, implemented, and tested in this paper as a convenient replacement for the conventional FT method in extracting data from received OOK-NRZ modulated signals. The proposed CNN model was trained using data that were collected experimentally using a 520 nm, 900 mW LD as an optical source that was operated at power values of 24, 26, and 27 dBm to test different scenarios. The modulated OOK-NRZ optical signals were transmitted in a tank full of Gulf seawater. The performance of the proposed CNN model

27 September 2023 11:31:04

© Author(s) 2023

and the conventional FTD approach based on channel conditions was compared. The proposed CNN model shows an outstanding improvement in recovering the originally transmitted data, with a substantial improvement achieved in terms of BER values. In addition, the effective channel length was extended approximately fourfold, and the transmitted SNR values required to achieve the MA-BER condition decreased by around 20 dB. Based on the results of this study, we can conclude that the proposed CNN model can improve the performance of UOWC systems without a mathematical formalization model or any *a priori* knowledge of channel conditions or characteristics.

AUTHOR DECLARATIONS

Conflict of Interest

The authors have no conflicts to disclose.

Author Contributions

Conceptualization, O. N. M. Salim; methodology, and formal analysis, O. N. M. Salim, S. A. Adnan, and A. H. Mutlag; investigation, O. N. M. Salim; resources, O. N. M. Salim, S. A. Adnan, and A. H. Mutlag; data curation, O. N. M. Salim, and A. H. Mutlag; writing original draft preparation, O. N. M. Salim; review and editing, S. A. Adnan, and A. H. Mutlag; supervision, S. A. Adnan, and A. H. Mutlag; funding acquisition, O. N. M. Salim. All authors have read and agreed to the published version of the manuscript.

Omar Nameer Mohammed Salim: Conceptualization (equal); Data curation (equal); Formal analysis (equal); Funding acquisition (equal); Investigation (equal); Methodology (equal); Project administration (equal); Resources (equal); Software (equal); Validation (equal); Writing – original draft (equal); Writing – review & editing (equal). **Salah A. Adnan**: Conceptualization (equal); Data curation (equal); Methodology (equal); Project administration (equal); Resources (equal); Supervision (equal); Validation (equal); Writing – review & editing (equal). **Ammar Hussein Mutlag**: Data curation (equal); Formal analysis (equal); Funding acquisition (equal); Methodology (equal); Project administration (equal); Resources (equal); Software (equal); Supervision (equal); Validation (equal); Writing – review & editing (equal).

DATA AVAILABILITY

The data that support the findings of this study are available from the corresponding author upon reasonable request.

REFERENCES

[1] S. A. Adnan, A. Alchalaby, and H. A. Hassan, "Future optimization algorithm to estimate attenuation in 532 nm laser beam of UWOC-channel: Improved neural network model," Math. Modell. Eng. Problems **8**, 453 (2021).

[2] S. A. Adnan, H. A. Hassan, A. Alchalaby, and A. C. Kadhim, "Experimental study of underwater wireless optical communication from clean water to turbid harbor under various conditions," Int. J. Des. Nature Ecodyn. **16**, 219 (2021).

[3] G. Cossu, R. Corsini, A. M. Khalid, S. Balestrino, A. Coppelli, A. Caiti, and E. Ciaramella, "Experimental demonstration of high speed underwater visible light communications," in *2013 2nd International Workshop on Optical Wireless Communications* (IEEE, 2013), Vol. 11.

[4] S. Adnan, M. Ali, and F. Hakwar, "The air bubbles effect for underwater optical wireless communication using 650 nm wavelength," Eng. Technol. J. **37**, 398 (2019).

[5] J. Wang, C. Lu, S. Li, and Z. Xu, "100 m/500 Mbps underwater optical wireless communication using an NRZ-OOK modulated 520 nm laser diode," Opt. Express **27**, 12171 (2019).

[6] P. Tian, X. Liu, S. Yi, Y. Huang, S. Zhang, X. Zhou, L. Hu, L. Zheng, and R. Liu, "High-speed underwater optical wireless communication using a blue GaN-based micro-LED," Opt. Express **25**, 1193 (2017).

[7] X. Yu, W. Jin, M. Sui, and Z. Lan, "Evaluation of forward error correction scheme for underwater wireless optical communication," in *2011 Third International Conference on Communications and Mobile Computing* (IEEE, 2011), Vol. 527.

[8] A. Liu, R. Zhang, B. Lin, and H. Yin, "Multi-degree-of-freedom for underwater optical wireless communication with improved transmission performance," J. Mar. Sci. Eng. **11**, 48 (2022).

[9] I. C. Ijeh, M. A. Khalighi, and S. Hranilovic, "Parameter optimization for an underwater optical wireless vertical link subject to link Misalignments," IEEE J. Oceanic Eng. **46**, 1424 (2021).

[10] J. Long, S. Xie, E. Li, C. Gao, Y. Gao, Y. Zhang, H. Zheng, G. Guo, and L. Huang, "Breakthrough the communication bottleneck between sky and underwater," AIP Adv. **11**, 025029 (2021).

[11] A. Jurado-Navas, N. G. Serrato, J. M. Garrido-Balsells, and M. Castillo-Vázquez, "Error probability analysis of OOK and variable weight MPPM coding schemes for underwater optical communication systems affected by salinity turbulence," OSA Continuum **1**, 1131 (2018).

[12] H. Yang, Q. Yan, M. Wang, Y. Wang, P. Li, and W. Wang, "Synchronous clock recovery of photon-counting underwater optical wireless communication based on deep learning," Photonics **9**, 884 (2022).

[13] X. Xu, Y. Li, P. Huang, M. Ju, and G. Tan, "BER performance of UWOC with APD receiver in wide range oceanic turbulence," IEEE Access **10**, 25203 (2022).

[14] Z. Chen, X. Tang, C. Sun, Z. Li, W. Shi, H. Wang, L. Zhang, and A. Zhang, "Experimental demonstration of over 14 AL underwater wireless optical communication," IEEE Photonics Technol. Lett. **33**, 173 (2021).

[15] F. Mattoussi, M. A. Khalighi, and S. Bourennane, "Improving the performance of underwater wireless optical communication links by channel coding," Appl. Opt. **57**, 2115 (2018).

[16] S. A. Adnan, M. A. Ali, A. C. Kadhim, M. Sadeq, and M. Riaz, "Investigating the performance of underwater wireless optical communication with intensity modulation direct detection technique," Light, Energy Environ. **JW5A**, 14 (2017).

[17] X. Tang, L. Zhang, C. Sun, Z. Chen, H. Wang, R. Jiang, Z. Li, W. Shi, and A. Zhang, "Underwater wireless optical communication based on DPSK modulation and silicon photomultiplier," IEEE Access **8**, 204676 (2020).

[18] M. V. Jamali, J. A. Salehi, and F. Akhoundi, "Performance studies of underwater wireless optical communication systems with spatial diversity: MIMO scheme," IEEE Trans. Commun. **65**, 1176 (2017).

[19] M. A. A. Ali, "Comparison of modulation techniques for underwater optical wireless communication employing APD receivers," Res. J. Appl. Sci. Eng. Technol. **10**, 707 (2015).

[20] W. C. Cox, J. A. Simpson, C. P. Domizioli, J. F. Muth, and B. L. Hughes, "An underwater optical communication system implementing Reed-Solomon channel coding," in *OCEANS 2008* (IEEE, 2008), Vol. 1.

[21] M. Doniec, I. Vasilescu, M. Chitre, C. Detweiler, M. Hoffmann-Kuhnt, and D. Rus, "AquaOptical: A lightweight device for high-rate long-range underwater point-to-point communication," in *OCEANS 2009* (IEEE, 2009), Vol. 1.

[22] H. Lin, H. Han, L. Ma, X. Zhang, and Z. Xiong, "Image enhancement for underwater range-gated image with multi-slice integration method," AIP Adv. **12**, 105016 (2022).

[23] L. Alzubaidi, J. Zhang, A. J. Humaidi, A. Al-Dujaili, Y. Duan, O. Al-Shamma, J. Santamaría, M. A. Fadhel, M. Al-Amidie, and L. Farhan, "Review of deep learning: Concepts, CNN architectures, challenges, applications, future directions," J. Big Data **8**, 53 (2021).

[24] X. Li, F. Dong, S. Zhang, and W. Guo, "A survey on deep learning techniques in wireless signal recognition," Wireless Commun. Mobile Comput. **2019**, 5629572.

27 September 2023 11:31:04

© Author(s) 2023

[25]O. N. Mohammed Salim, " New neuro-fuzzy system-based holey polymer fibers drawing process," AIP Adv. **7**, 105301 (2017).
[26]C. Li, X. Wei, H. Guo, W. He, X. Wu, H. Xu, and X. Liu, "Recognition of the internal situation of aircraft skin based on deep learning" AIP Adv. **11**, 105216 (2021).
[27]C. El Mazgualdi, T. Masrour, N. Barka, and I. El Hassani, "Learning-based decision tool towards smart energy optimization in the manufacturing process," Systems **10**, 180 (2022).
[28]S. Yang, Y. Hou, Y. Shang, and X. Zhong, "BPNN and CNN-based AI modeling of spreading and icing pattern of a water droplet impact on a supercooled surface," AIP Adv. **12**, 045209 (2022).
[29]N. Jmour, S. Zayen, and A. Abdelkrim, *Convolutional Neural Networks for Image Classification* (IC_ASET) (IEEE, 2018), p. 397.
[30]Z. Xing, Y. Liu, Q. Wang, and J. Li, "Multi-sensor signals with parallel attention convolutional neural network for bearing fault diagnosis," AIP Adv. **12**, 075020 (2022).
[31]C. Zheng, S. Yu, and W. Gu, "A SVM-based processor for free-space optical communication," in *2015 IEEE 5th ICEIEC* (IEEE, 2015), p. 30.
[32]R. A. Mohammed, O. N. M. Salim, A. H. Al-Nakkash, and A. A. S. Alabdullah, "Proposed APs distribution optimization algorithm: Aware of interference (APD-AI)," IOP Conf. Ser.: Mater. Sci. Eng. **745**, 012040 (2020).
[33]H. Ye, G. Y. Li, and B.-H. Juang, "Power of deep learning for channel estimation and signal detection in OFDM systems," IEEE Wireless Commun. Lett. **7**, 114 (2018).
[34]F. Zou, Z. Liu, X. Hu, and G. Wang, "A novel PAPR reduction scheme for OFDM systems based on neural networks," Wireless Commun. Mobile Comput. **2021**, 5574807.
[35]J. Li, M. Zhang, D. Wang, S. Wu, and Y. Zhan, "Joint atmospheric turbulence detection and adaptive demodulation technique using the CNN for the OAM-FSO communication," Opt. Express **26**, 10494 (2018).
[36]F. N. Khan, K. Zhong, X. Zhou, W. H. Al-Arashi, C. Yu, C. Lu, and A. P. T. Lau, "Joint OSNR monitoring and modulation format identification in digital coherent receivers using deep neural networks," Opt. Express **25**, 17767 (2017).
[37]Q. Tian, C. Lu, B. Liu, L. Zhu, X. Pan, Q. Zhang, L. Yang, F. Tian, and X. Xin, "DNN-based aberration correction in a wavefront sensorless adaptive optics system," Opt. Express **27**, 10765 (2019).
[38]Z. Li and X. Zhao, "BP artificial neural network based wave front correction for sensor-less free space optics communication," Opt. Commun. **385**, 219 (2017).
[39]J. Thrane, J. Wass, M. Piels, J. C. M. Diniz, R. Jones, and D. Zibar, "Machine learning techniques for optical performance monitoring from directly detected PDM-QAM signals," J. Lightwave Technol. **35**, 868 (2017).
[40]M. A. Amirabadi, M. H. Kahaei, S. A. Nezamalhosseini, and V. T. Vakili, "Deep learning for channel estimation in FSO communication system," Opt. Commun. **459**, 124989 (2020).
[41]L. Darwesh and N. S. Kopeika, "Deep learning for improving performance of OOK modulation over FSO turbulent channels," IEEE Access **8**, 155275 (2020).
[42]M. Uysal, C. Capsoni, Z. Ghassemlooy, A. Boucouvalas, and E. Udvary, *Optical Wireless Communications: An Emerging Technology* (Springer International Publishing, 2016).
[43]onsemi, Introduction to the silicon photomultiplier (SiPM) - AND9770/D, Semiconductor Components Industries LLC, 2021, 2011, 13.
[44]M. T. Dabiri, S. M. S. Sadough, and M. A. Khalighi, "FSO channel estimation for OOK modulation with APD receiver over atmospheric turbulence and pointing errors," Opt. Commun. **402**, 577 (2017).
[45]F. Li and H. Lu, "*Optimum detection threshold for free-space optical communication with atmospheric scintillation*," in *2015 International Conference on Optoelectronics and Microelectronics (ICOM)* (IEEE, 2016), p. 191.
[46]M. A. Fakhri, Z. H. Tawfiq, and S. A. Adnan, "Gold nanoparticles in ethanol deposited on PCF for refractive index sensors," AIP Conf. Proc. **2213**, 020245 (2020).
[47]B. Barua, "Comparison the performance of free-space optical communication with OOK and BPSK modulation under atmospheric turbulence," Int. J. Eng. Sci. Technol. **3**, 4391 (2011).
[48]R. Cai, M. Zhang, D. Dai, Y. Shi, and S. Gao, "Analysis of the underwater wireless optical communication channel based on a comprehensive multiparameter model," Appl. Sci. **11**, 6051 (2021).
[49]W.-H. Shin, J.-Y. Choi, and S.-K. Han, "Fixed threshold on-off keying differential detection for satellite optical communications," Opt. Express **27**, 1590 (2019).
[50]O. N. M. Salim, A. H. Mutlag, S. A. Adnan, and S. Q. Mahdi, "Design and experimental study of an efficient controlled cooling system for optical communication laser diodes," Math. Modell. Eng. Problems **9**, 779 (2022).
[51]I. Goodfellow, Y. Bengio, and A. Courville, *Deep Learning* (MIT Press, 2016).
[52]Y. Kutsumi, N. Kanegawa, M. Zeida, H. Matsubara, and N. Murayama, "Automated bowel sound and Motility analysis with CNN using a smartphone" Sensors **23**, 407 (2022).

27 September 2023 11:31:04

© Author(s) 2023